Sekban, D. M., Yıldız, H. (2024). Investigation Mechanical Properties of Weld Zone High Strength AH32 Shipbuilding Steel Joined by Shielded Metal Arc, Gas Metal Arc and Submerged Arc Welding Methods. *The Black Sea Journal of Sciences*, 14(4), 1873-1887.

The Black Sea Journal of Sciences, 14(4), 1873-1887, 2024. DOI: 10.31466/kfbd.1501344

KFBD

Karadeniz Fen Bilimleri Dergisi
The Black Sea Journal of Sciences
ISSN (Online): 2564-7377 https://dergipark.org.tr/tr/pub/kfbd

Araştırma Makalesi / Research Article

Investigation Mechanical Properties of Weld Zone High Strength AH32 Shipbuilding Steel Joined by Shielded Metal Arc, Gas Metal Arc and Submerged Arc Welding Methods

Dursun Murat SEKBAN[1*], Hacı YILDIZ[2]

Abstract

Ships are built by joining steels of varying strength values using a welding method. While low-medium strength steels are advantageous in terms of low cost and easy supply, high strength steels provide a significant advantage in terms of being preferred in shipbuilding with the high strength values they offer. Examining the welding of steels used in shipbuilding reveals that while several welding techniques are employed, shielded metal arc welding (SMAW), submerged arc welding (SAW) and gas metal arc welding (GMAW) are most frequently used. Examination of the literature indicates that the aforementioned welding procedures have been employed relatively little in studies on the joining of high-strength steels used in ship construction. Also, it has been noted that no research has been done on the comparative analysis of the mechanical characteristics of such steels when they are joined using these 3 welding techniques. In this study, SMAW, GMAW, and SAW are used to join AH32 steel, which is often used in shipbuilding, and the mechanical characteristics of the welding areas are compared. Examinations revealed that SAW produced the greatest results in terms of bending force, hardness, strength, and impact toughness. Following GMAW, the best results were also obtained in terms of bending and tensile elongation.

Keywords: Shipbuilding steels, Shielded metal arc welding, Gas metal arc welding, Submerged arc welding, Mechanical properties.

Örtülü Elektrod Ark Kaynağı, Gazaltı Kaynağı ve Tozaltı Kaynağı ile Birleştirilen Yüksek Mukavemetli AH32 Gemi İnşa Çeliğinin Mekanik Özelliklerinin Karşılaştırmalı İncelenmesi

Öz

Gemiler, çeşitli dayanım değerlerine sahip çeliklerin kaynak yöntemiyle birleştirilmesiyle inşa edilir. Düşük-orta dayanımlı çelikler düşük maliyet ve tedarik kolaylığı açısından avantajlıyken, yüksek dayanımlı çelikler sundukları yüksek dayanım değerleriyle gemi inşaatında avantaj sağlamaktadırlar. Gemi inşasında kullanılan çeliklerin kaynakları incelendiğinde, çeşitli kaynak teknikleri kullanılmakla birlikte, en sık örtülü elektrot ark kaynağı, tozaltı kaynağı ve gazaltı kaynağının kullanıldığı görülmektedir. Literatür incelendiğinde, gemi inşasında kullanılan yüksek mukavemetli çeliklerin birleştirilmesine yönelik çalışmaların oldukça sınırlı olduğu görülmektedir. Ayrıca literatürde bu tür çeliklerin bu 3 kaynak tekniği kullanılarak birleştirildiğindeki mekanik özelliklerinin karşılaştırmalı analizi üzerine herhangi bir araştırma yapılmadığı da belirlenmiştir. Bu bağlamda bu çalışmada gemi yapımında yaygın olarak kullanılan AH32 çeliği örtülü elektrot ark kaynağı, tozaltı kaynağı ve gazaltı kaynağı ile birleştirilerek kaynak bölgelerinin çeşitli mekanik özellikleri incelenmiştir. İnceleme sonrasında sertlik, akma dayanımı, çekme dayanımı, darbe tokluğu ve eğilme dayanımı açısından en iyi sonuçların tozaltı kaynağı sonrasında, çekme uzaması ve eğilme uzaması açısından ise en iyi değerlerin gazaltı kaynağı sonrası elde edildiği belirlenmiştir.

Anahtar Kelimeler: Gemi inşaatı çeliği, Örtülü elektrod ark kaynağı, Gazaltı kaynağı, Tozaltı kaynağı, Mekanik özellikler.

[1]Department of Marine Engineering Operations, Karadeniz Technical University, Trabzon, Turkey, msekban@ktu.edu.tr
[2]Directorate of Maritime Affairs, BOTAŞ LNG Operations, Tekirdag, Turkey, haciyildiz86@hotmail.com

[*]Sorumlu Yazar/Corresponding Author
Geliş/Received: 14.06.2024 **Kabul/Accepted:** 11.11.2024 **Yayın/Published:** 15.12.2024

1. Introduction

Ships are built from a wide variety of materials, including steel, polyethylene, aluminum alloys, composite materials, and wood. However, particularly in the building of commercial ships it is evident that steels are more popular because of their exceptional strength and formability (Sekban et al., 2016). Steels used in shipbuilding may be divided into two primary categories: high strength steels and low-medium strength steels. High strength steels are recommended for ship types and ship parts where high strength is required, even though low-medium strength steels stand out for having qualities like excellent weldability and easy availability. When the high-strength steels used in ship construction are examined, it is seen that especially AH-32, AH-36, DH-32, DH-36, EH-32, EH-36 and HSLA steels come to the fore in terms of usage and the studies in the literature focus on the weldability of these steels (Kim et al., 2008, Zou et al., 2018b, Cunha et al., 2019, Wu et al., 2023, Pankaj et al., 2020, Zou et al., 2018a, Zhong et al., 2023, Yuan et al., 2022b, Konkol et al., ., 2003, Zou et al., 2020, Zhang et al., 2019, Donizete Borba et al., 2017, Yuan et al., 2022a, Xie et al., 2021, Zhang et al., 2022, Tiwari et al., 2019, Unt et al. , 2015, Cater et al., 2016). In the studies, steels frequently used in ship construction were successfully joined with different welding methods and the mechanical properties in the welding areas were examined in detail. The investigations' findings revealed that the strength and hardness values in the welding metal (WM) were often higher than those in the base material and that these values generally showed a negative trend as one moved from the WM to the heat-affected zone (HAZ).

As it is known, ships are formed by welding steels which cut and shaped in various lengths. Conventional arc welding procedures such as shielded metal arc welding (SMAW), gas metal arc welding (GMAW), gas tungsten arc welding (GTAW) and submerged arc welding (SAW) stand out in terms of frequency of use in joining steels in various industries including the shipbuilding industry (Serindağ & Çam, 2021; Şenol & Çam, 2023; Ezer & Çam, 2022; Serindağ & Çam, 2022; Serindağ & Çam, 2023; Serindağ et al., 2022). While GMAW is preferred because it can be applied to many different material groups, SMAW is preferred because it can enter narrow spaces, and SAW is generally preferred especially in the welding of thick plates due to its ability to reach high current values. Even though each welding technique has several benefits and drawbacks, it is reasonable to argue that these three techniques are the most often utilized in shipyards because of their numerous overall benefits.

Though few, studies on the employment of the aforementioned welding techniques to weld different types of steel used in shipbuilding are found in the literature (Görgün, 2024, Cho et al., 1999, Yılmaz and Tümer, 2013, Sönmez and Ceyhun, 2014, Çolak et al., 2019, Mert et al., 2016, Hariprasath et al., 2022, Khamari et al., 2020, Ragu Nathan et al., 2023, Ahmed et al., 2022, Yıldız

et al., 2023, Pratikno et al., 2021). Furthermore, very little research has been done on the mechanical characterization of the WM of AH-32 steel, which is usually chosen in shipbuilding because of its high strength, using any of these welding techniques (Kim et al., 2004, Lima Junior, 2018). On the other hand, no study in the literature comparatively examines the mechanical properties of the welded joints of AH-32 steel produced with SMAW, GMAW and SAW, which are widely used in ship construction. As it is known, the mechanical properties of the structure formed in the welding area after welding are of great importance. In this context, it is very important to determine the mechanical properties of the structure formed after welding, such as hardness, strength, impact toughness and bending strength. AH-32 high strength shipbuilding steel was welded using SMAW, GMAW, and SAW in this study's context—a first in the literature—and the values of the welding area's hardness, strength, impact strength, and bending strength were compared.

2. Materials and Methods

In the studies, AH32 shipbuilding steel was used, the chemical composition of which is given in Table 1. The plates prepared with dimensions of 125 mm X 250 mm and thickness of 8 mm were welded and some images of welded structures are given in Figure 1.

Table 1. The chemical composition of the steel and the parameters used during the welding.

Chemical Composition of AH 32 Shipbuilding Steel										
C	Mn	P	S	Si	Ni	Cu	Cr	V	Mo	Fe
0,19	0,8	0,03	0,035	0,25	0,45	0,3	0,21	0,06	0,07	Balance

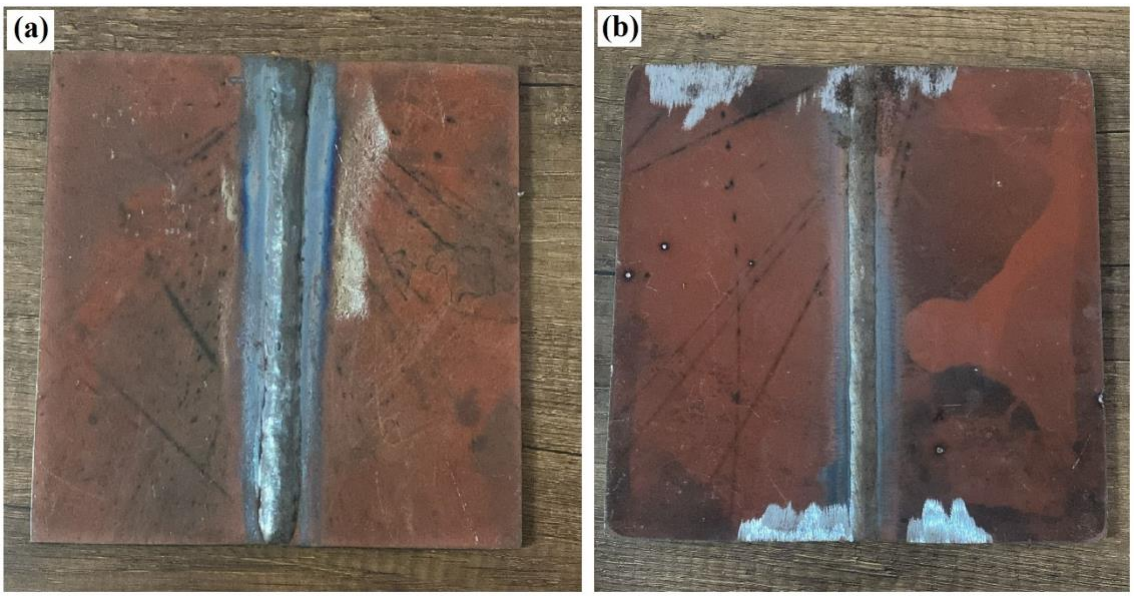

Figure 1. Images of welded structures: (a) gas metal arc welding and (b) submerged arc welding.

The parameters used during welding are shown in Table 2. SMAW and SAW joints were performed on both sides, whereas in GMAW was performed on one side since ceramic substrate was used. During the welding process, no additional metal other than the welding electrode is used. During double-sided SMAW and SAW, a welding mouth was not opened on the first side surface to be welded. After welding the first surface, the back side was turned and a thin mouth was opened with a grinding machine in this part and welding operations were carried out on this side. For all type welds tack welding was applied at 100 mm intervals to fix the parts in the correct position during the welding process. In the SMAW ESB 48 electrode, in the GMAW TS EN ISO 17632-A standard electrode and during SAW TS EN ISO 14171-A standard electrode was used. On the other hand, CO_2 was used as the shielding gas in the GMAW, and basic powders were used as the shielding powder in the SAW.

Table 2. Welding parameters.

Welding Parameters			
Welding Type	Wire Diameter (mm)	Current Value (A)	Voltage Value (V)
SMAW	3	120	30
GMAW	1.6	210	32
SAW	4	600	32

As seen in Figure 2, hardness, tensile, impact toughness and bending test samples were taken after the welding processes. In the hardness tests carried out using the Vickers hardness method on a Duramin brand hardness measurement unit at room temperature, a load of 300 g and a waiting time of 10 seconds under load were used. Hardness scans of the welding areas of the samples were carried out horizontally at 1 mm intervals, starting from 1 mm below the surface. Tensile experiments were carried out on an Instron 3382 brand universal tensile device at room temperature and a deformation rate of 5x10-4 s^{-1}. During the test, two different test samples were used, one containing the base material in the tensile zone (big tensile sample) and one without (small tensile sample), as shown in Figure 2. Dimensions of small-sized tensile samples extracted from the welding zone is 3 mm x 4 mm x 27 mm. On the other hand, the tensile test samples containing the main structure in the tensile area prepared according to the ASTM E8M standard are 13 mm x 4 mm x 52 mm. Tensile tests were performed at least 3 times for both sample types for each welding technique, and stress-strain curves were created by averaging the obtained values. The impact toughness values of the welded structures after each welding were determined with the average values obtained in the impact tests performed at least 3 times at room temperature. The samples used in the impact tests were prepared in size 3 mm x 4 mm x 27 mm according to the KLST DIN 50115 (miniaturized specimens) standard. Bending tests were performed at room temperature on an Instron 3382 brand test machine. The tests were

performed with samples prepared according to the ASTM E 190 standard with measuring 2 mm x 7 mm x 32 mm. The samples were subjected to bending force at a jaw speed of 1 mm/min during the test. At least three samples for each case were subjected to bending testing during room temperature testing, and the graph and table show the average of the data.

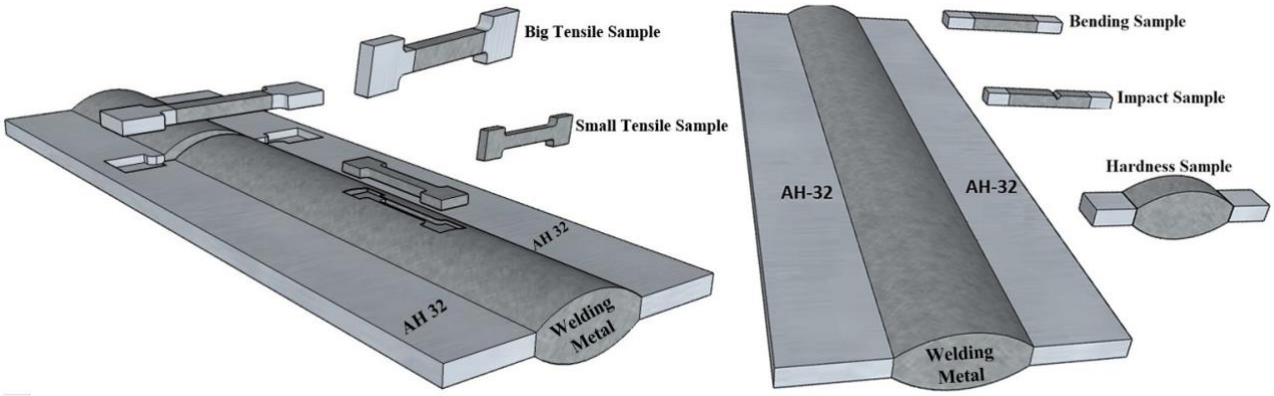

Figure 2. Schematics illustrations of samples removed from welded plates.

3. Findings and Discussion

3.1. Heat Input Calculations

The following formulation was used to calculate the heat inputs during the welding process and the heat inputs were determined. The current and voltage values used during welding were included in the formulation as set values, and the thermal efficiency values were selected as 0.8 for SMAW and GMAW and 1 for SAW. Welding speeds were determined by measuring the time during welding.

$$Heat\ Input = \frac{\text{Arc Voltage x Arc Current x Thermal Efficiency}}{\text{Travel Speed}} \quad (1)$$

As expected after the calculations, the highest heat input values were obtained after SAW as seen in Table 3. On the other hand, although the GMAW and SMAW heat inputs were close to each other, slightly lower heat input values were calculated after GMAW.

Table 3. Heat input values occurring during welding.

Welding Type	Heat Input (kj/mm)
SMAW	0.594
GMAW	0.574
SAW	1.089

3.2. Hardness

Figure 3 shows the distribution of hardness values horizontally from the weld center in the samples removed from the welded plates. As a result of the examinations, it is seen that the hardness value of 169 HV in the base material increases in the WM after every 3 weld types. When the average hardness values in the WM are compared, the lowest values were reached in SMAW welding with 182 HV. Also, while an average hardness of 208 HV was obtained in WM after GMAW, this value increased to 231 HV after SAW. It is believed that the quick cooling that follows high temperatures is the primary cause of the highest hardness value after SAW. (Lee et al., 2014). On the other hand, although the heat input during GMAW is lower than in SMAW, the main reason for obtaining higher hardness values is thought to be the controlled heat input caused by the gas protection during welding and the higher quality weld seam resulting from this. It is observed that in all three weld types, the reduced heat input leads to comparatively lower hardness values when the moves outside the WM zone. Also the hardness values in all weld types decline and approach the base material's hardness value of 169 HV when we move outside the HAZ.

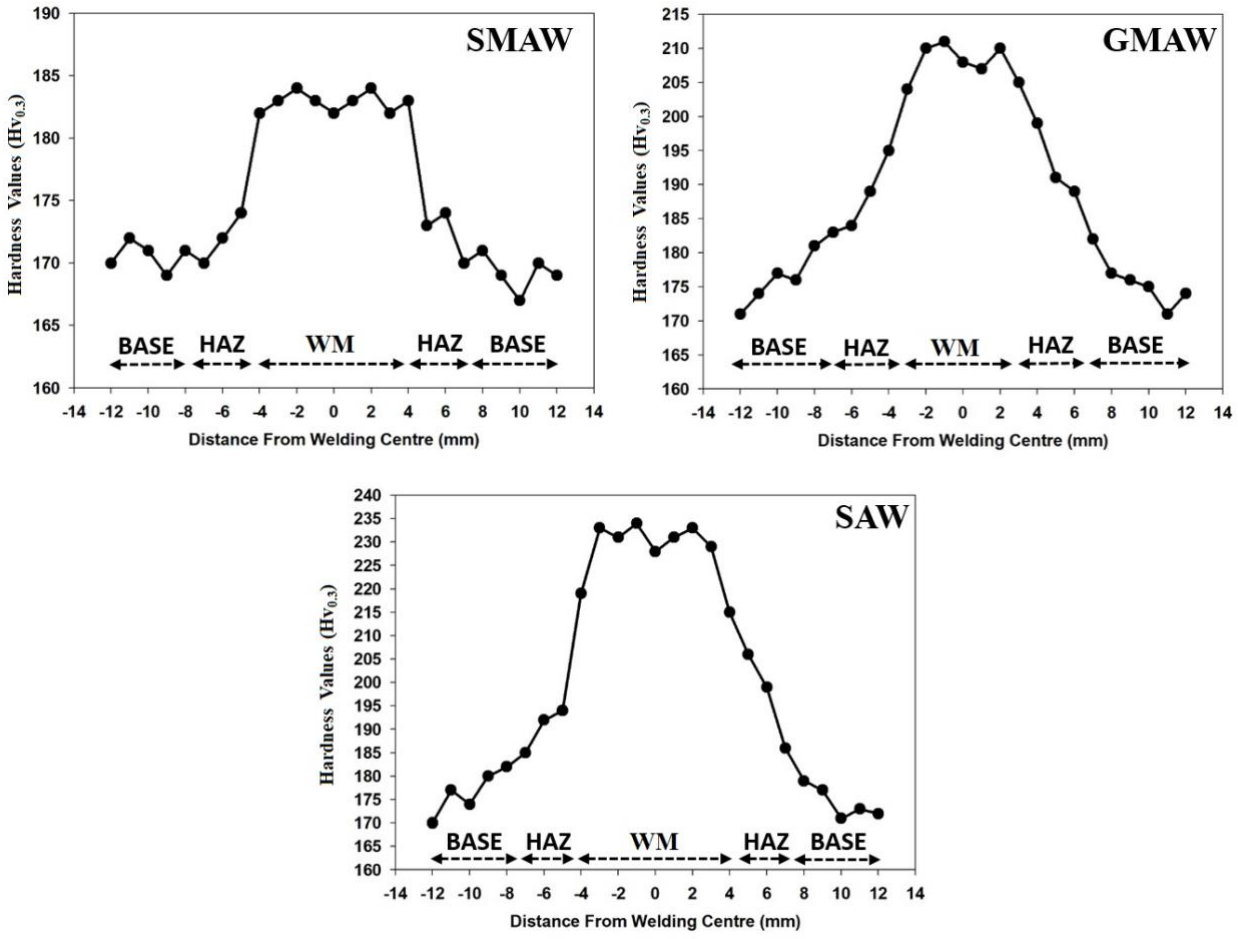

Figure 3. Variation of hardness values after welding according to weld type.

3.3. Strength

The curve representing the change in strength and elongation values in the WM after welding, as well as the values generated from this curve, are shown in Figure 4 and Table 4, respectively. The strength values in the WM increased following the application of all welding types. So much so that the yield strength value of the base AH32, which was 367 MPa, increased to 396 MPa after SMAW, 427 MPa after GMAW and 437 MPa after SAW. While the tensile strength values were 564 MPa in the base material, it increased to 611 MPa after SMAW, 679 MPa after GMAW and 697 MPa after SAW. It is believed that the structures generated as a result of cooling following the high temperatures attained during welding are what explain this rise in strength levels after welding (Conte et al., 2023, Mahala, 2019). The relatively high temperature reached in submerged arc welding and the subsequent high cooling rates lead to the formation of relatively highest strength values after this welding method. On the other hand, as can be seen in Figure 4 and Table 4, the elongation values in the base material decreased after all welding methods. The total elongation value, measured as 33.8% in the main structure, decreased to 31.7% after SMAW, 30.1% after GMAW and 27.8% after SAW. It is believed that the inhibitory influence of the changes in grain size and morphology after the attained temperature and cooling is what causes this fall in elongation values after welding (Soleymani et al., 2012).

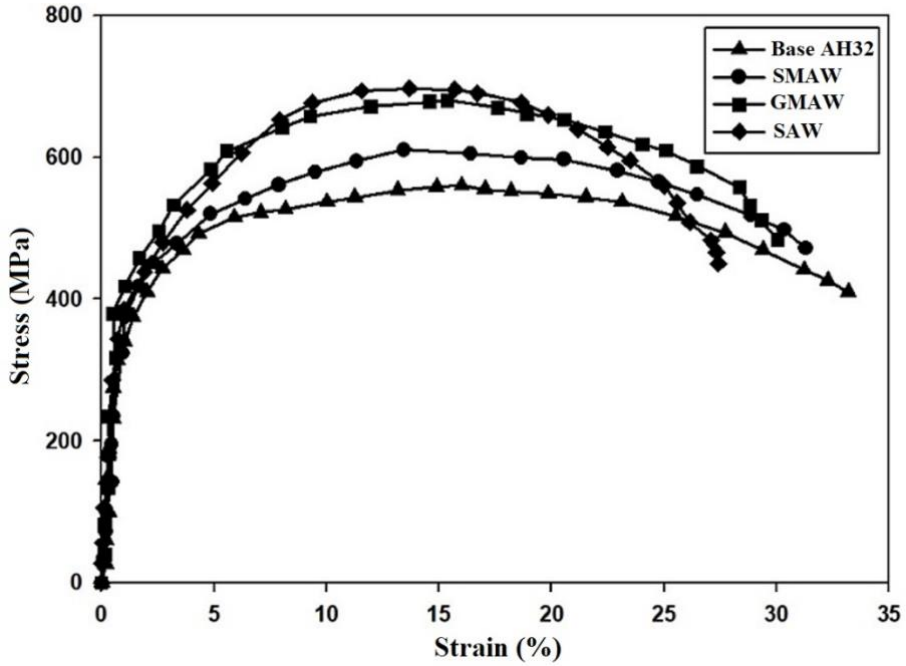

Figure 4. Strength and elongation curves of the welded samples (completely removed from the welding area) and base AH32 steel.

Table 4. Strength and elongation curves of the welded samples (completely removed from the welding area) and base AH32 steel.

Condition	Yield Strength (MPa)	Tensile Strength (MPa)	Total Elongation (%)
Base AH32 Steel	367 ± 07	564 ± 12	33,8 ± 1,7
SMAW	396 ± 10	611 ± 09	31,7 ± 1,3
GMAW	427 ± 14	679 ± 16	30,1 ± 2,4
SAW	437 ± 09	697 ± 13	27,8 ± 2,1

Strength and elongation values only for the WM were determined by using small-sized tensile samples that did not include the base material in the gauge length region. Therefore, within the scope of the study, large-sized tensile samples, including the base material in the gauge length region, were removed from the samples subjected to welding processes and these samples were subjected to tensile tests. In this way, it was determined in which regions the deformation would occur in the loads that may be applied to the welded samples. The strength-strain curves of the tests performed are shown in Figure 5 and the values obtained from these curves are shown in Table 5. During all of the samples prepared in the figure, it was seen that the ruptures were not from the weld metal region, but from the base material. As can be seen from the curves and tables, while there was no significant change in the strength values of the samples as the samples broke away from the base material, there was a significant decrease in the amount of elongation. The reason for this situation is the difference in yield strength between the base material and the welded zone. During the tensile test, deformation occurs throughout the entire dimension of the sample consisting entirely of the base material, while only the base material undergoes deformation in the samples including the welded zone. While the gauge length in the samples consists of both the base material and the welded zone, only the base material largely contributes to the elongation during the experiment. As a result, the total elongation rate in the samples decreases significantly compared to that of the sample consisting entirely of the base material. (Çam et al., 1998, Çam et al., 1997, Kim et al., 2001).

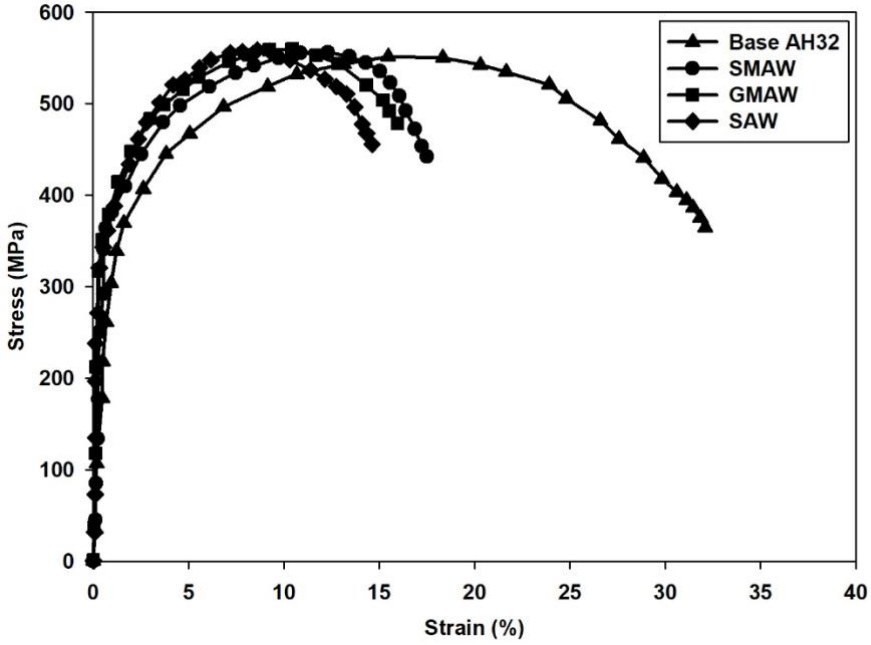

Figure 5. Strength and elongation curves of the welded samples (including the both base and welded zone in the gauge length) and base AH32 steel.

Table 5. Strength and elongation curves of the welded samples (including the both base and welded zone in the gauge length) and base AH32 steel.

Condition	Yield Strength (MPa)	Tensile Strength (Mpa)	Total Elongation (%)
Base AH32 Steel	361 ± 09	552 ± 14	32,4 ± 1,9
SMAW	366 ± 12	556 ± 11	17,6 ± 1,4
GMAW	362 ± 15	562 ± 15	16,1 ± 2,1
SAW	371 ± 08	558 ± 19	14,9 ± 1,6

3.4. Impact Toughness

The visuals of the impact toughness determined in WM for all 3 welding methods after the impact tests and the table containing the obtained values are shown in Figure 6 and Table 6, respectively. The impact toughness value, which was 9.4 J in the base material, rose to 11.1 J following SMAW, 12.9 J following GMAW, and 12.5 J following SAW. The change in the fracture energy of AH32 steel depending on the welding method is due to the fact that each method has different thermal and metallurgical properties. In GMAW, the protective gas environment reduces oxidation and produces a more uniform and fine-grained microstructure, resulting in high fracture energy. It is also thought that the low level of internal stresses resulting from the relatively low heat input during GMAW may also lead to higher impact strength. In SAW, deep penetration and high strength are achieved with high heat input, while it is thought that the fracture energy level remains

low compared to gas metal arc welding after relatively low elongation values. On the other hand after SMAW, the effect of the slag layer and relatively low welding speed can cause relatively larger grains to form in the microstructure and increase internal stresses. This situation leads to a decrease in fracture strength and explains the relatively lower fracture energy obtained in welding with SMAW.

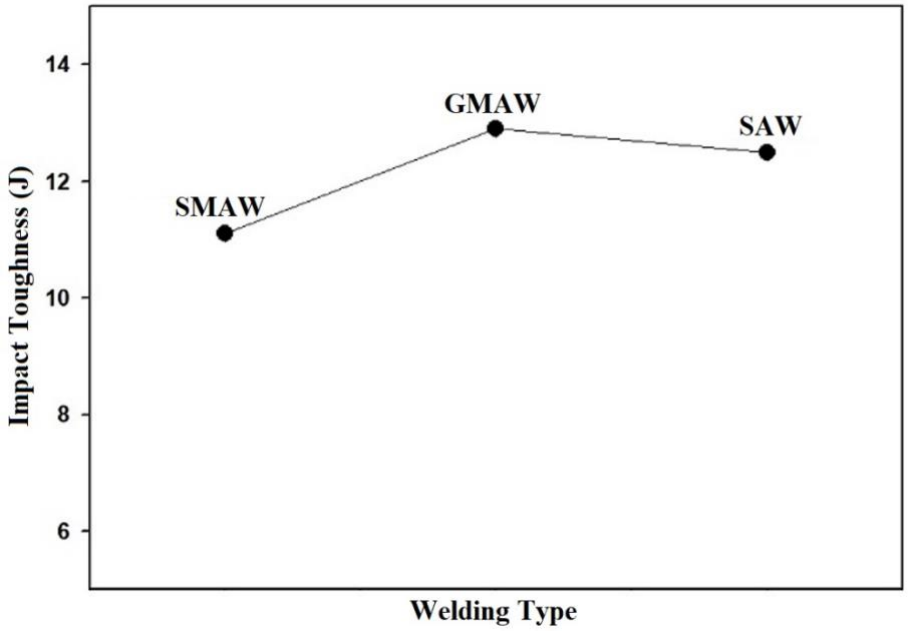

Figure 6. Variation of impact toughness values after welding according to welding type.

Table 6. Impact toughness values obtained in the base material and weld zones.

Condition	Impact Toughness (J)
Base AH32 Steel	9,4 ± 0,4
SMAW	11,1 ± 0,7
GMAW	12,9 ± 0,6
SAW	12,5 ± 0,8

3.5. Bending

The formability of welded structures is of great importance and this feature is generally determined by bending tests in welded structures. Figure 7 and Table 7 display the curve, which depicts the change in bending force and bending elongation values in the weld zone following welding, and the values derived from this curve, respectively. 486 N bending force value in the base AH32 steel increased in parallel with the increase in strength in the welded structures and increased to 517 N after SMAW, 598 N after GMAW and 633 N after SAW. The deflection values at the maximum bending force decreased after welding, in parallel with the decreasing elongation values after all welding methods. On the other hand, when the welding methods are examined among

themselves, the highest bending force values are reached after submerged arc welding, where the highest strength value is formed, while the lowest values in bending elongation also occur after this welding method. Among the welding methods, the lowest bending force and highest bending elongation values occurred after welding with shielded metal arc welding. It is thought that GMAW exhibits higher strength values in bending tests due to the finer grain structure in the welded area, lower internal stresses and clean weld seam due to the lower heat input and gas protection compared to SMAW.

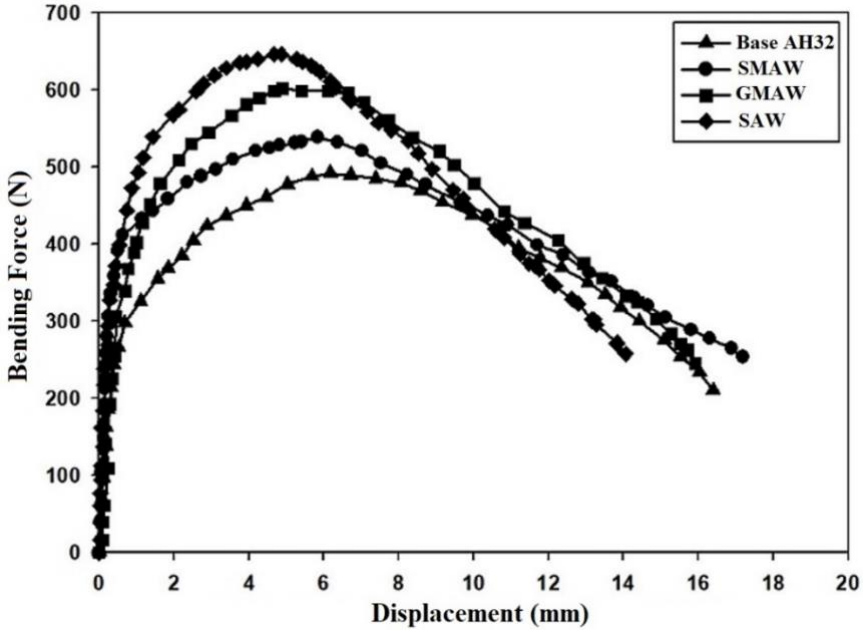

Figure 7. Variation of bending force after welding and bending elongation at maximum force depending on the welding type.

Table 7. Bending force and displacement values obtained in the base material and weld zones.

Condition	Bending Force (N)	Displacement at Maximum Bending Force (mm)
Base AH32 Steel	486 ± 12	6,7 ± 0,4
SMAW	517 ± 14	6,2 ± 0,7
GMAW	598 ± 10	5,7 ± 0,6
SAW	633 ± 16	5,1 ± 0,4

4. Conclusions

In the study, high-strength AH-32 steel, which is widely used in shipbuilding, was joint with shielded metal arc welding, gas metal arc welding and submerged arc welding, and the mechanical properties of the welding zone were investigated comparatively. As a result of the investigations, the results summarized below were reached:

1- The highest hardness value in WM was reached after submerged arc welding with 231 HV.

2- After all three welds, strength values increased in WM and the highest strength value was reached in the submerged arc weld with 437 MPa. On the other hand, after all 3 welds, the elongation at break values reached in the WM decreased compared to the base AH32.

3- In the tests performed with tensile samples including the base material deformation occurred in the base material region. After tests no significant changes were observed in the strength values compared to the base AH32 steel. Also, in the tests performed with these samples, it was determined that the elongation values decreased in all welding methods.

4- The highest impact toughness value was reached after gas metal arc welding with 12.9 Joules.

5- After the bending tests applied to welded joints, the highest bending force was reached after submerged arc welding with 633 N.

Authors' Contributions

All authors contributed equally to the study.

Statement of Conflicts of Interest

There is no conflict of interest between the authors.

Statement of Research and Publication Ethics

The authors declares that this study complies with Research and Publication Ethics.

References

Ahmed, M. M. Z., El-Sayed Seleman, M. M., Touileb, K., Albaijan, I., & Habba, M. I. A. (2022). Microstructure, Crystallographic Texture, and Mechanical Properties of Friction Stir Welded Mild Steel for Shipbuilding Applications. Materials 15(8): 2905.

Cater, S., Martin, J., Galloway, A., & McPherson, N. (2016). Comparison between Friction Stir and Submerged Arc Welding Applied to Joining DH36 and E36 Shipbuilding Steel. In R. Mishra, M. W. Mahoney, Y. Sato, Y. Hovanski, & R. Verma (Eds.), Friction Stir Welding and Processing VII (pp. 49-58). Cham: Springer International Publishing.

Cho, K.-K., Sun, J.-G., & Oh, J.-S. (1999). An automated welding operation planning system for block assembly in shipbuilding. International Journal of Production Economics 60-61: 203-209. doi:https://doi.org/10.1016/S0925-5273(98)00151-0

Conte, R., Izquierdo, D.R. & Francesco, G. Submerged arc welding process: a numerical investigation of temperatures, displacements, and residual stresses in ASTM A516-Gr70 corner joined samples. Int J Adv Manuf Technol 127, 5437–5448 (2023). https://doi.org/10.1007/s00170-023-11908-x

Cunha, P. H. C. P. d., Lemos, G. V. B., Bergmann, L., Reguly, A., Santos, J. F. d., Marinho, R. R., & Paes, M. T. P. (2019). Effect of welding speed on friction stir welds of GL E36 shipbuilding steel. Journal of Materials Research and Technology 8(1): 1041-1051. doi:https://doi.org/10.1016/j.jmrt.2018.07.014

Çam, G., Yeni, Ç., Erim, S., Ventzke, V., & Koçak, M. (1998). Investigation into properties of laser welded similar and dissimilar steel joints. Sci. Technol. Weld. Join., 3 (4): 177-189. doi:https://doi.org/10.1179/stw.1998.3.4.177

Çam, G., Koçak, M., Dobi, D., Heikinheimo, L., & Siren, M. (1997). Fracture behaviour of diffusion bonded bimaterial Ti-Al joints. Sci. Technol. Weld. Join., 2 (3): 95-101. doi:https://doi.org/10.1179/stw.1997.2.3.95

Çolak, Z., Ayan, Y., & Kahraman, N. (2019). Gerçek deniz ortamında su altı kaynağı ile birleştirilen Grade AH36 gemi sacının kaynak bölgesinin karakterizasyonu. Gazi Üniversitesi Mühendislik Mimarlık Fakültesi Dergisi, 35(2), 775-786. https://doi.org/10.17341/gazimmfd.519055

Donizete Borba, T. M., Duarte Flores, W., de Oliveira Turani, L., & Cardoso Junior, R. (2017). Assessment of the Weldability of EH36 TMCP Shipbuilding Steel Welded by High Heat Input Submerged Arc Welding. Welding International 31(3): 184-195. doi:10.1080/09507116.2016.1218619

Ezer, M. & Çam, G. (2022). A Study on microstructure and mechanical performance of gas metal arc welded AISI 304L joints. Materialwissenschaft und Werkstofftechnik 53 (9): 1043-1052. doi:https://doi.org/10.1002/mawe.202200050

Görgün, E. (2024). Investigation of The Effect of SMAW Parameters On Properties of AH36 Joints And The Chemical Composition of Seawater. International Journal of Innovative Engineering Applications, 8(1), 28-36. https://doi.org/10.46460/ijiea.1418641

Hariprasath, P., Sivaraj, P., Balasubramanian, V., Pilli, S., & Sridhar, K. (2022). Effect of the welding technique on mechanical properties and metallurgical characteristics of the naval grade high strength low alloy steel joints produced by SMAW and GMAW. CIRP Journal of Manufacturing Science and Technology 37: 584-595. doi:https://doi.org/10.1016/j.cirpj.2022.03.007

Khamari, B. K., Dash, S. S., Karak, S. K., & Biswal, B. B. (2020). Effect of welding parameters on mechanical and microstructural properties of GMAW and SMAW mild steel joints. Ironmaking & Steelmaking 47(8): 844-851. doi:10.1080/03019233.2019.1623592

Kim, H., Kim, I., Kim, I., & Kang, B. (2008). Control of welding process for BV-AH 32 steel. Archives of Materials Science 46, 46.

Kim, J. H., Oh, Y. J., Hwang, I. S., Kim, D. J., & Kim, J. T. (2001). Fracture behavior of heat-affected zone in low alloy steels. Journal of Nuclear Materials, 299(2), 132-139. https://doi.org/10.1016/S0022-3115(01)00688-2

Konkol, P. J., Mathers, J. A., Johnson, R., & Pickens, J. R. (2003). Friction Stir Welding of HSLA-65 Steel for Shipbuilding. Journal of Ship Production 19(03): 159-164. doi:10.5957/jsp.2003.19.3.159

Lee, J. H., Park, S. H., Kwon, H. S., Kim, G. S., & Lee, C. S. (2014). Laser, tungsten inert gas, and metal active gas welding of DP780 steel: Comparison of hardness, tensile properties and fatigue resistance. Materials & Design 64: 559-565. doi:https://doi.org/10.1016/j.matdes.2014.07.065

Mahala, T. (2019). Gas Metal Arc Welding By Taguchi Technique. Journal of Emerging Technologies and Innovative Research 6 (3): 107-109

Mert, T., Bilgili, L., Senoz, K. M., Çelebi, U. B., & Ekinci, S. (2016). The Effect of Parameter Selection on Fume Formation Rate in SMAW of AH36 Shipbuilding Steel and Analysis with ANOVA Method. In P. Grammelis (Ed.), Energy, Transportation and Global Warming (pp. 795-802). Cham: Springer International Publishing.

Pankaj, P., Tiwari, A., Biswas, P., Rao, A. G., & Pal, S. (2020). Experimental studies on controlling of process parameters in dissimilar friction stir welding of DH36 shipbuilding steel–AISI 1008 steel. Welding in the World 64(6): 963-986. doi:10.1007/s40194-020-00886-3

Pratikno, H., Pahlawan, N. A., & Dhanista, W. L. (2021). Comparative Analysis of FCAW, and GMAW Welding With Heat Input Variations on A36 Steel Against Vickers Hardness Test and Macrostructure. International Journal of Offshore and Coastal Engineering (IJOCE) 5(2): 59-61

Ragu Nathan, S., Balasubramanian, V., Rao, A. G., Sonar, T., Ivanov, M., & Suganeswaran, K. (2023). Effect of tool rotational speed on microstructure and mechanical properties of friction stir welded DMR249A high strength low alloy steel butt joints for fabrication of light weight ship building structures.

International Journal of Lightweight Materials and Manufacture 6(4): 469-482. doi:https://doi.org/10.1016/j.ijlmm.2023.05.004

Sekban, D. M., Aktarer, S. M., Xue, P., Ma, Z. Y., & Purcek, G. (2016). Impact toughness of friction stir processed low carbon steel used in shipbuilding. Materials Science and Engineering: A 672: 40-48. doi:https://doi.org/10.1016/j.msea.2016.06.063

Serindağ, H.T. & Çam, G. (2021). Microstructure and mechanical properties of gas metal arc welded AISI 430/AISI 304 dissimilar stainless steels butt joints. Journal of Physics: Conference Series, 1777: 012047. doi:https://doi.org/10.1088/1742-6596/1777/1/012047

Serindağ, H.T. & Çam, G. (2022). Multi-pass butt welding of thick AISI 316L plates by gas tungsten arc welding: Microstructural and mechanical characterization. International Journal of Pressure Vessels and Piping, 200: 104842. doi: https://doi.org/10.1016/j.ijpvp.2022.104842

Serindağ, H.T. & Çam, G. (2023). Characterizations of microstructure and properties of dissimilar AISI 316L/9Ni low alloy cryogenic steel joints fabricated by GTAW. Journal of Materials Engineering and Performance 32: 7039-7049. doi: https://doi.org/10.1007/s11665-022-07601-x

Serindağ, H.T., Tardu, C., Kirçiçek, I.Ö, & Çam, G. (2022). A study on microstructural and mechanical properties of gas tungsten arc welded thick cryogenic 9% Ni alloy steel butt joint. CIRP Journal of Manufacturing Science and Technology, 37: 1-10. doi:https://doi.org/10.1016/j.cirpj.2021.12.006

Soleymani, V. & Eghbali, B. (2012). Grain Refinement in a Low Carbon Steel Through Multidirectional Forging. Journal of Iron and Steel Research, International 19 (10): 74-78. https://doi.org/10.1016/S1006-706X(12)60155-1

Sönmez, U., & Ceyhun, V. (2014). Investigation of mechanical and microstructural properties of S 235 JR (ST 37-2) steels welded joints with FCAW. Kovove Materialy-Metallic Materials 52: 57-63

Şenol, M. & Çam, G. (2022). Investigation into microstructures and properties of AISI 430 ferritic steel butt joints fabricated by GMAW. International Journal of Pressure Vessels and Piping, 202: 104926. doi:https://doi.org/10.1016/j.ijpvp.2023.104926

Tiwari, A., Pankaj, P., Biswas, P., Kore, S. D., & Rao, A. G. (2019). Tool performance evaluation of friction stir welded shipbuilding grade DH36 steel butt joints. The International Journal of Advanced Manufacturing Technology 103(5): 1989-2005. doi:10.1007/s00170-019-03618-0

Unt, A., Poutiainen, I., & Salminen, A. (2015). Influence of Filler Wire Feed Rate in Laser-Arc Hybrid Welding of T-butt Joint in Shipbuilding Steel with Different Optical Setups. Physics Procedia 78: 45-52. doi:https://doi.org/10.1016/j.phpro.2015.11.016

Wu, Y., Yuan, X., Kaldre, I., Zhong, M., Wang, Z., & Wang, C. (2023). TiO2-Assisted Microstructural Variations in the Weld Metal of EH36 Shipbuilding Steel Subject to High Heat Input Submerged Arc Welding. Metallurgical and Materials Transactions B 54(1): 50-55. doi:10.1007/s11663-022-02697-x

Xie, X., Zhao, T., Zhao, H., Li, S., & Wang, C. (2021). Heterogeneous Microstructure-Induced Mechanical Responses in Various Sub-Zones of EH420 Shipbuilding Steel Welded Joint Under High Heat Input Electro-Gas Welding. Acta Metallurgica Sinica (English Letters) 34(10): 1427-1433. doi:10.1007/s40195-021-01245-x

Yıldız, N. B., Gürol, U., Baykal, H., Koçak, M. (2023). Sualtında Birleştirilen AH36 Gemi Sacının Mikro Yapı ve Mekanik Özelliklerinin İncelenmesi. Mühendis Ve Makina, 64(710), 1-16. https://doi.org/10.46399/muhendismakina.1027899

Yılmaz, R., & Tümer, M. (2013). Microstructural studies and impact toughness of dissimilar weldments between AISI 316 L and AH36 steels by FCAW. The International Journal of Advanced Manufacturing Technology 67(5): 1433-1447. doi:10.1007/s00170-012-4579-0

Yuan, X., Wu, Y., Zhong, M., Basu, S., Wang, Z., & Wang, C. (2022). Profiling inclusion characteristics in submerged arc welded metals of EH36 shipbuilding steel treated by CaF2–TiO2 fluxes. Science and Technology of Welding and Joining 27(8): 683-690. doi:10.1080/13621718.2022.2095589

Yuan, X., Zhong, M., Wu, Y., & Wang, C. (2022). Characterizing Inclusions in the Weld Metal of EH36 Shipbuilding Steel Processed by CaF2-30 Wt Pct TiO2 Flux. Metallurgical and Materials Transactions B 53(2): 656-661. doi:10.1007/s11663-022-02455-z

Zhang, J., Leng, J., & Wang, C. (2019). Tuning Weld Metal Mechanical Responses via Welding Flux Optimization of TiO2 Content: Application into EH36 Shipbuilding Steel. Metallurgical and Materials Transactions B 50(5): 2083-2087. doi:10.1007/s11663-019-01645-6

Zhang, Y., Zhang, J., Liu, H., Wang, Z., & Wang, C. (2022). Addressing Weld Metal Compositional Variations in EH36 Shipbuilding Steel Processed by CaF2-SiO2-CaO-TiO2 Fluxes. Metallurgical and Materials Transactions B 53(3): 1329-1334. doi:10.1007/s11663-022-02480-y

Zhong, M., Jiang, L., Bai, H.-y., Basu, S., Wang, Z.-j., & Wang, C. (2023). Simulating molten pool features of shipbuilding steel subjected to submerged arc welding. Journal of Iron and Steel Research International 30(3): 569-579. doi:10.1007/s42243-022-00908-y

Zou, X.-d., Sun, J.-c., Zhao, D.-p., Matsuura, H., & Wang, C. (2018). Effects of Zr addition on evolution behavior of inclusions in EH36 shipbuilding steel: from casting to welding. Journal of Iron and Steel Research International 25(2): 164-172. doi:10.1007/s42243-018-0022-6

Zou, X., Sun, J., Matsuura, H., & Wang, C. (2020). Unravelling Microstructure Evolution and Grain Boundary Misorientation in Coarse-Grained Heat-Affected Zone of EH420 Shipbuilding Steel Subject to Varied Welding Heat Inputs. Metallurgical and Materials Transactions A 51(3): 1044-1050. doi:10.1007/s11661-019-05604-3

Zou, X., Zhao, D., Sun, J., Wang, C., & Matsuura, H. (2018). An Integrated Study on the Evolution of Inclusions in EH36 Shipbuilding Steel with Mg Addition: From Casting to Welding. Metallurgical and Materials Transactions B 49(2): 481-489. doi:10.1007/s11663-017-1163-x